SUPPLEMENTAL INFORMATION

Analyzing resistance to design selective chemical inhibitors for AAA proteins

Rudolf Pisa[1, 2, 4], Tommaso Cupido[1, 4], Jonathan B Steinman[1, 3], Natalie H Jones[1, 2] and Tarun M Kapoor[1,5] *

[1]Laboratory of Chemistry and Cell Biology, The Rockefeller University, New York, NY 10065, USA.

[2]Tri-Institutional PhD Program in Chemical Biology, The Rockefeller University, New York, NY 10065, USA.

[3]Tri-Institutional MD-PhD Program, The Rockefeller University, New York, NY 10065, USA.

[4]These authors contributed equally.

[5]Lead contact.

*Correspondence: kapoor@rockefeller.edu

Table S1. Crystallography data collection and refinement statistics. Related to Figures 2 and 4.

spastin-AAA:	N527C	T692A	WT	T692A	T692A
ligand:	compound **1**	compound **1**	compound **4**	compound **4** form A	compound **4** form B
pdbID:	**6P10**	**6P11**	**6P12**	**6P13**	**6P14**
Data collection					
Space group	$P6_5$	$P6_5$	$P6_5$	$P6_5$	$P6_5$
Cell dimensions					
a, b, c (Å)	79.4 79.4 97.3	79.5 79.5 97.2	80.9 80.9 96.3	79.7 79.7 96.9	105.3 105.3 65.4
α, β, γ (°)	90, 90, 120	90, 90, 120	90, 90, 120	90, 90, 120	90, 90, 120
Resolution (Å)	50.0-2.30 (2.34-2.30)	50.0-2.15 (2.19-2.15)	50.0-1.94 (1.97-1.94)	50.0-2.10 (2.14-2.10)	50.0-1.93 (1.96-1.93)
Wavelength (Å)	0.9181	0.9201	0.9197	0.9201	0.9201
R_{merge}	0.044 (0.468)	0.035 (0.391)	0.031 (0.450)	0.043 (0.448)	0.039 (0.439)
$<I>/\sigma I$	32.2 (1.8)	37.4 (2.7)	52.5 (2.8)	42.0 (2.7)	40.7 (2.9)
Completeness (%)	99.0 (99.5)	99.8 (99.9)	99.0 (99.2)	99.9 (100.0)	99.9 (100.0)
Multiplicity	4.7 (4.1)	5.5 (5.6)	6.5 (6.7)	5.8 (6.0)	5.8 (6.0)
Total reflections	71736	103752	168901	118576	180192
Unique reflections	15364 (783)	18985 (940)	26138 (1323)	20435 (1015)	31137 (1549)
CC1/2	100 (81.9)	99.39 (89.6)	99.6 (91.3)	99.4 (86.9)	99.8 (90.6)
Refinement					
Resolution (Å)	39.7-2.30 (2.38-2.30)	39.7-2.15 (2.23-2.15)	40.34 – 1.94 (2.01-1.94)	39.85 – 2.10 (2.18-2.10)	34.47 – 1.93 (1.99 – 1.93)
No. reflections	15360 (1546)	18944 (1878)	26123 (2613)	20389 (2020)	31108 (3101)
No. refl. for R_{free}	1548 (147)	1889 (189)	2615 (265)	2048 (203)	3091 (306)
R_{work} / R_{free}	0.206/0.252	0.213/0.241	0.193 / 0.230	0.207 / 0.245	0.179 / 0.200
No. atoms	2120	2291	2354	2208	2199
Protein	2044	2046	2095	2059	1979
Ligands/ions	40	67	41	41	49
Water	36	178	218	108	171
B-factors					
Protein	61.51	55.31	48.00	50.54	43.94
Ligand/ion	64.98	52.86	44.57	45.94	42.02
Water	62.46	63.29	57.14	55.78	46.83
R.m.s. deviations					
Bond lengths (Å)	0.003	0.002	0.003	0.002	0.019
Bond angles (°)	0.64	0.44	0.58	0.49	1.58
Clashscore	4.40	4.12	4.77	1.94	2.51
Rotamer Outliers	1.00	0.00	0.98	0.00	2.05
Ramachandran Favored (%)	96.34	96.69	98.90	97.06	97.67
Ramachandran Allowed (%)	3.66	3.31	1.10	2.94	2.33
Ramachandran Outliers (%)	0.00	0.00	0.00	0.00	0.00

*Data in brackets indicate the high-resolution shell.

A

[compound **1**], (μM)	k_{cat}	Hill coeff.	$K_{1/2}$
40	n.d.	n.d.	n.d.
20	n.d.	n.d.	n.d.
10	3.1 (0.6)	2.5 (0.2)	1.4 (0.1)
5	3.0 (0.3)	2.8 (0.2)	0.8 (0.1)
2.5	3.5 (0.4)	2.6 (0.2)	0.5 (0.1)
1.25	3.6 (0.6)	2.2 (0.1)	0.4 (0.1)
DMSO	3.5 (0.03)	2.2 (0.2)	0.2 (0.01)

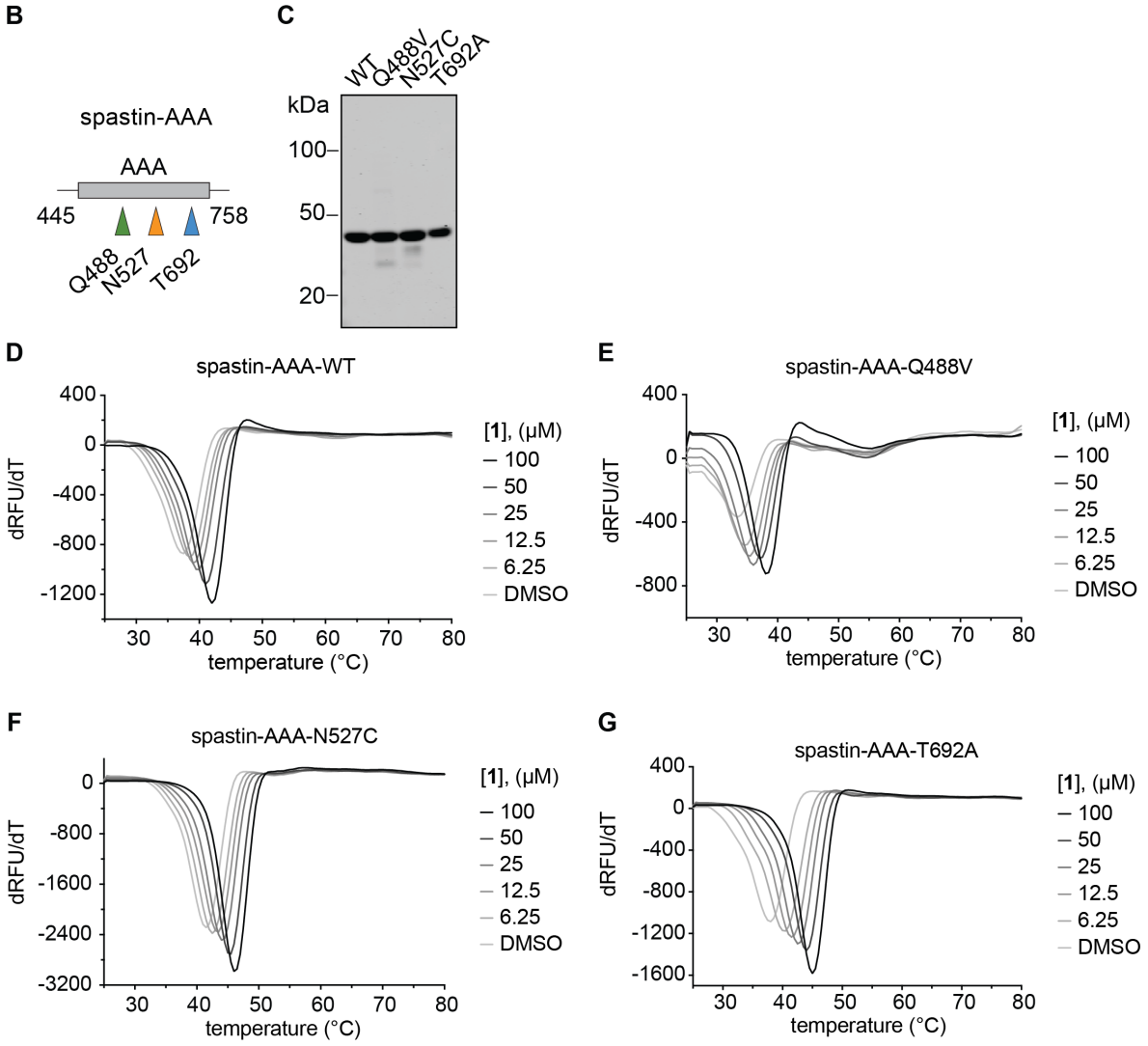

Figure S1. Related to Figure 1.

(A) ATP concentration-dependence of the steady-state ATPase activity of spastin-WT (*Drosophila melanogaster* spastin, aa 209-758, see Methods for details) at different concentrations of compound **1**, analyzed using a steady-state NADH-coupled assay. To calculate enzyme parameters, rates were plotted against ATP concentration and data were fit to the Michaelis-Menten equation for cooperative enzymes.

Range of ATP concentrations tested was 0.04 to 2.5 mM. The data from each experiment were fit separately and the values determined by the fitting were averaged. Values for apparent enzyme activity parameters including k_{cat}, Hill coefficient and $K_{1/2}$ are provided (average, s.d. in parentheses, n=3). n.d. = not determined. (B) Schematic shows the AAA domain (gray box) of the truncated recombinant construct (*Drosophila melanogaster* spastin-AAA, aa 445-758, see Methods for details). The positions of three variability hot-spot residues are highlighted (arrows). The first and last residues of the construct are also numbered. (C) SDS-PAGE analysis (Coomassie blue) of purified spastin-AAA-WT and constructs with mutations in variability hot-spot residues (Q488V, N527C, and T692A). (D-G) Differential scanning fluorimetry analysis of the melting temperature of spastin-AAA constructs in the presence of compound **1** (Supporting data for Figure 1E). Data from one representative experiment are shown for each construct (n=2; spastin-AAA-WT, -Q488V, -N527C and T692A).

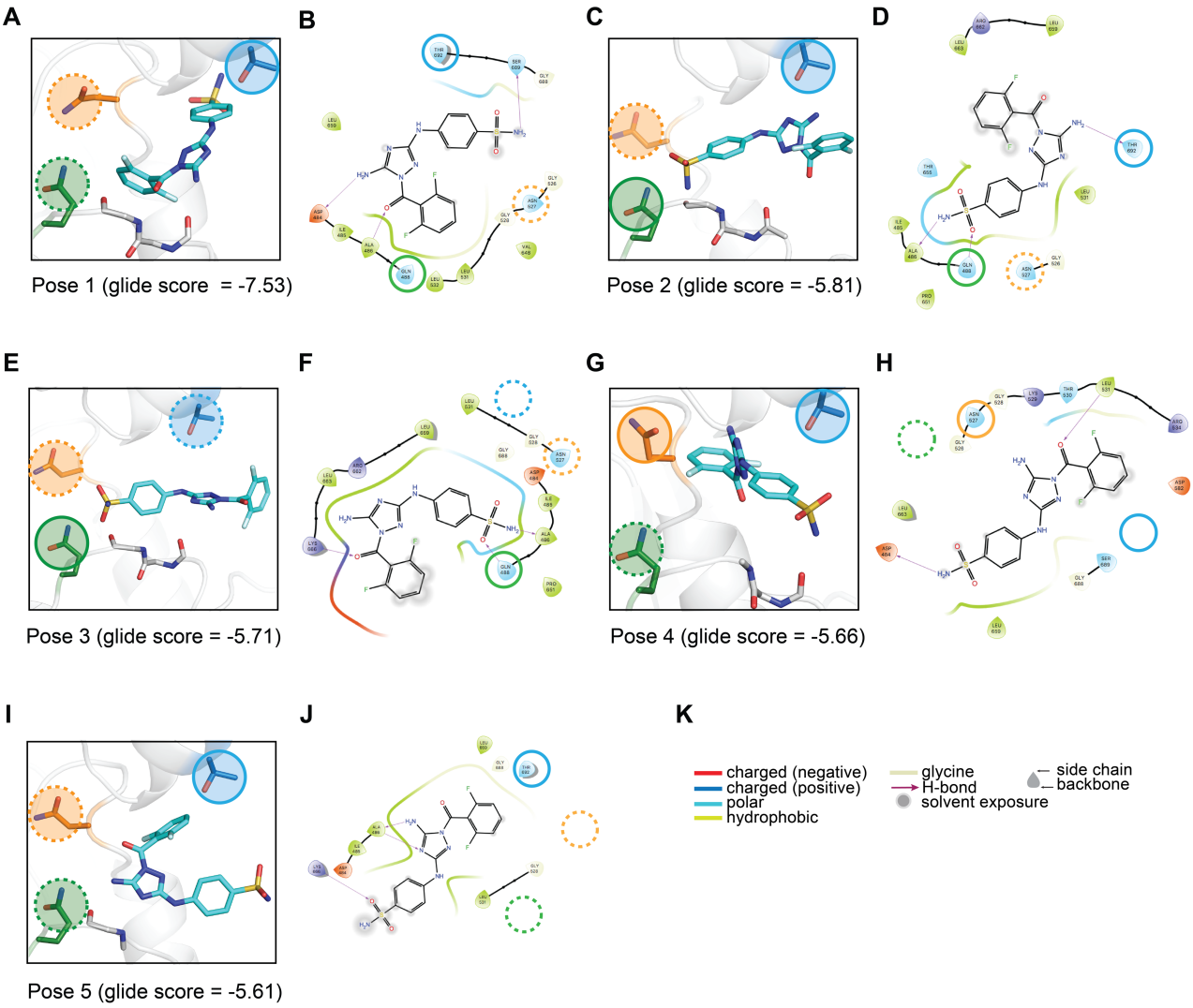

Figure S2. Related to Figure 1.

(A-J) Computational docking models for compound **1** bound to spastin. Five top scoring poses for compound **1** docked in the ATP site of spastin are shown (A, C, E, G and I). See Methods for details how these models were generated. Interaction maps for each pose are also shown (B, D, F, H and J; for details see panel K). The expected positions of the variability hotspot residues are highlighted by circles (Q488 – green, N527 – orange, T692 – blue; residue-compound distance < 4 Å: full circle, > 4 Å: dotted circle). Pose 5 (Figure S2I, J) is also shown in Figure 1G.

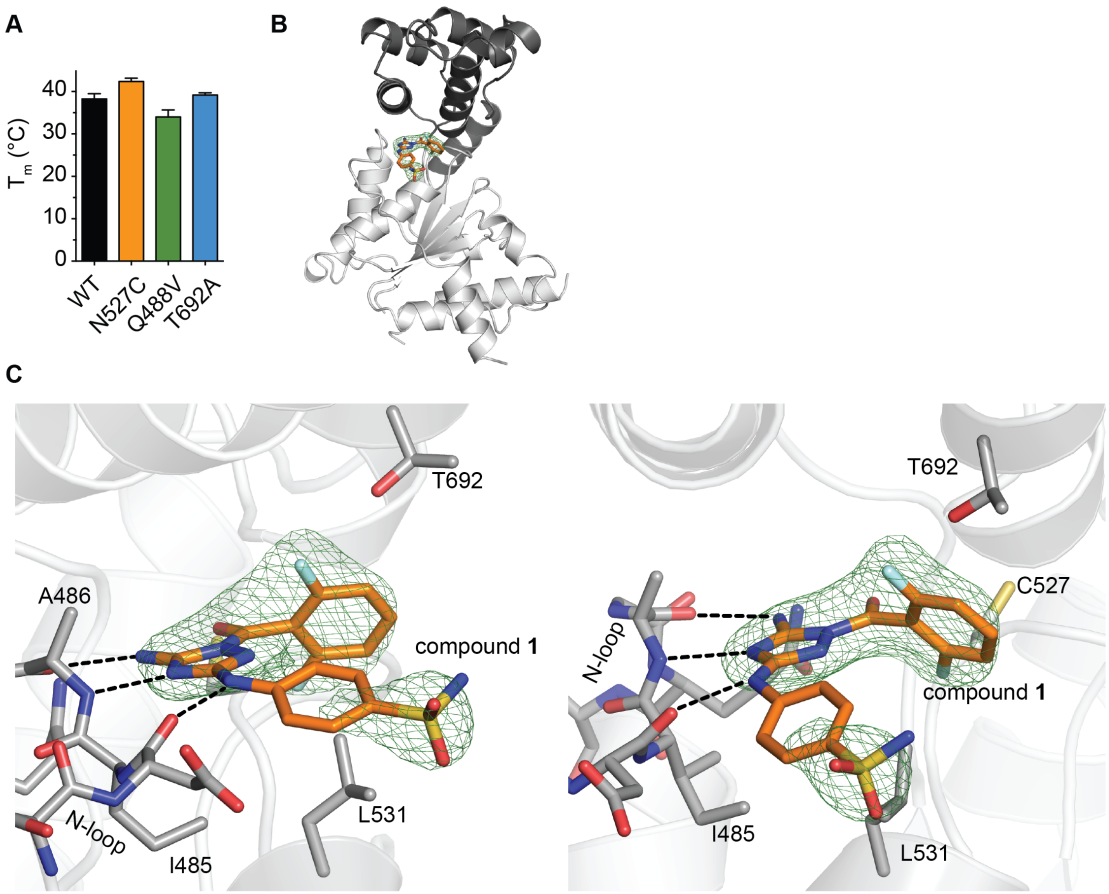

Figure S3. Related to Figure 2.

(A) Melting temperature of spastin-AAA-WT, -Q488V, -N527C and T692A constructs analyzed using differential scanning fluorimetry (n = 3; observed T_m for spastin-AAA-WT: ~38.5°C; -N527C: ~42°C; -Q488V: ~34.5°C; -T692A: ~39°C). (B) Crystal structure of spastin-AAA-N527C-compound **1** complex. Spastin's AAA domain (ribbon representation, gray) and compound **1** (stick representation, orange) are shown. Composite omit electron density around the compound is also shown (contoured at 3σ, green mesh). (C) Two views of spastin-AAA-N527C-compound **1** complex. Simulated annealing omit electron density map around compound **1** contoured at 3σ is shown (green mesh). Predicted hydrogen-bonding network between compound **1** and spastin's N-loop is also shown (black dashed lines).

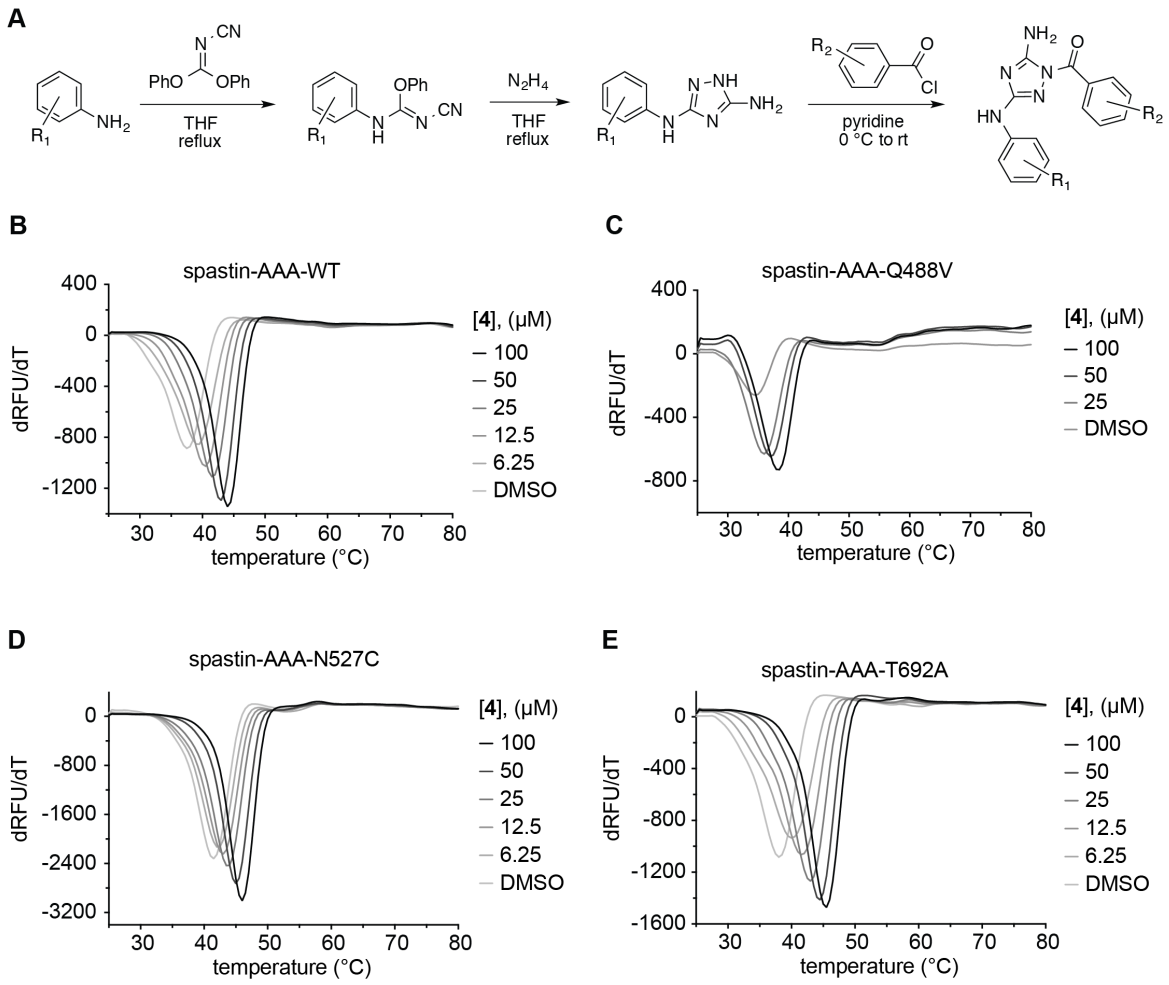

Figure S4. Related to Figure 3.

(A) Schematic for the synthesis of compound **1** analogs (adapted from Malerich et al, 2010). (B-E) Differential scanning fluorimetry analysis of the melting temperature of spastin-AAA constructs (spastin-AAA-WT, -Q488V, -N527C and -T692A) in the presence of compound **4** (Supporting data for Figure 3D, n=2). Data from one representative experiment are shown for each construct.

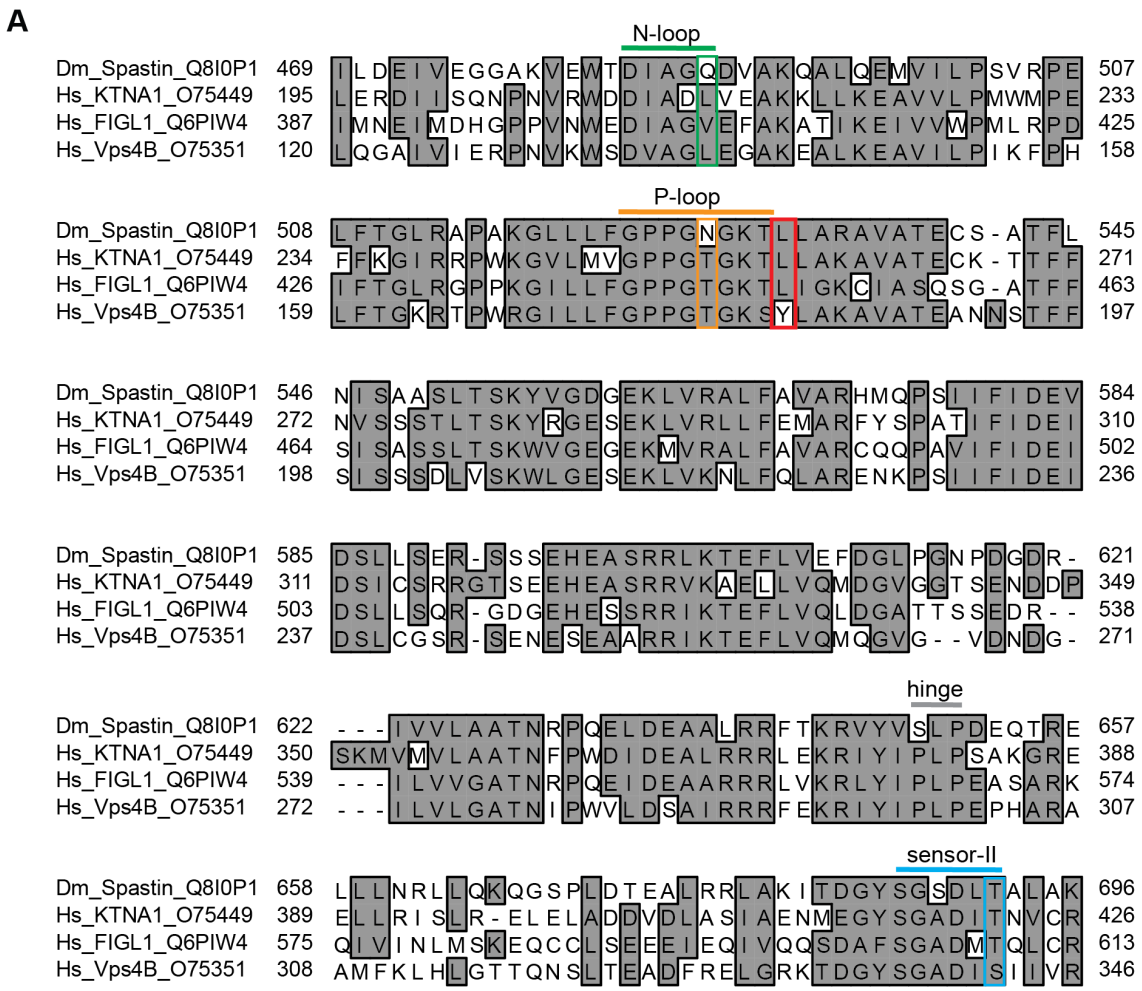

Figure S5. Related to Figure 3.

(A) Sequence alignment of the AAA domains of *D. melanogaster* spastin, human katanin, human FIGL1 and human VPS4B proteins (supporting data for Figure 3F). Conserved ATP binding motifs are highlighted (N-loop, P-loop, hinge and sensor-II). Residues at the entrance of the ATP pocket are indicated (red box). Variability hot-spot residues in the N-loop (green), P-loop (orange), hinge (gray) and sensor-II motifs (blue) are also indicated by colored boxes.

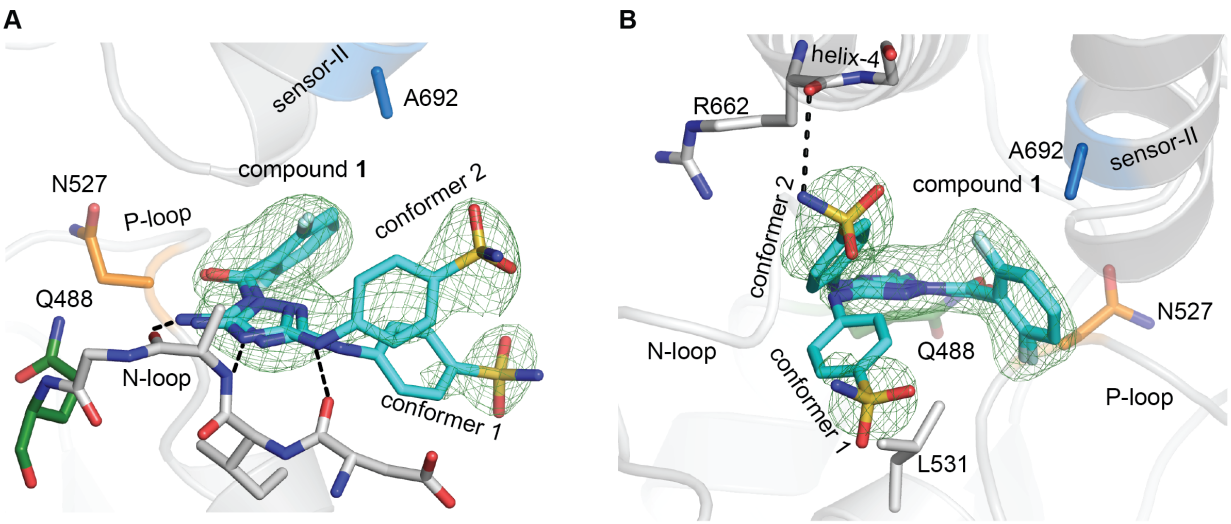

Figure S6. Two views of compound **1** in the active site of spastin-AAA-T692A. Related to Figure 5. (A) View of compound **1**, the N-loop motif and the side chains of variability hot-spot residues in the active site of spastin (Gln-488, green; Asn-527, orange; T692A, blue). (B) View of compound **1** from the entrance of the ATP binding site. Potential interaction of the compound **1**'s phenylsulfonamide moiety (conformer 2) with the residue in helix 4 of the small AAA subdomain (Arg-662) is highlighted (black dashed line).